Nuclear Modification Factor of Neutral Pions in the Forward and Backward Regions in *p*-Pb Collisions

R. Aaij *et al.*[*]
(LHCb Collaboration)

(Received 25 April 2022; accepted 10 June 2022; published 24 July 2023)

The nuclear modification factor of neutral pions is measured in proton-lead collisions collected at a center-of-mass energy per nucleon of 8.16 TeV with the LHCb detector. The π^0 production cross section is measured differentially in transverse momentum (p_T) for $1.5 < p_T < 10.0$ GeV and in center-of-mass pseudorapidity ($\eta_{\mathrm{c.m.}}$) regions $2.5 < \eta_{\mathrm{c.m.}} < 3.5$ (forward) and $-4.0 < \eta_{\mathrm{c.m.}} < -3.0$ (backward) defined relative to the proton beam direction. The forward measurement shows a sizable suppression of π^0 production, while the backward measurement shows the first evidence of π^0 enhancement in proton-lead collisions at the LHC. Together, these measurements provide precise constraints on models of nuclear structure and particle production in high-energy nuclear collisions.

DOI: 10.1103/PhysRevLett.131.042302

Neutral pion production is an important probe of nuclear effects in heavy ion collisions. In proton-lead (p-Pb) collisions at the Large Hadron Collider (LHC), π^0 production is particularly sensitive to cold nuclear matter (CNM) effects on the initial state of the bound nucleons in the colliding nucleus. Pion production in p-Pb collisions can be described using the collinear factorization framework where CNM effects are encoded into nuclear parton distribution functions (NPDFs) [1–4] and the parton-parton collision dynamics are described by perturbative quantum chromodynamics (PQCD) [5]. These NPDFs are determined using fits to data and are poorly constrained for partons with momentum fraction x smaller than about 10^{-4}. At low x and low momentum transfer Q, the parton number density may become so large that parton saturation effects become sizable. Parton saturation would lead to nonlinear evolution of parton densities and is often described using the color glass condensate (CGC) effective field theory [6]. Measurements of π^0 production in p-Pb collisions at forward and backward rapidities with the LHCb detector can provide constraints on NPDFs for x between 10^{-6} and 10^{-1}, potentially helping identify the onset of parton saturation effects [7].

Measurements of angular correlations in small-collision systems at the LHC [8–12] and the Relativistic Heavy Ion Collider (RHIC) [13,14] show evidence of collective flow, which cannot be described using only collinear factorization and NPDFs. In addition, the LHCb experiment recently measured the nuclear modification factor of inclusive charged particles in p-Pb collisions at a center-of-mass energy per nucleon of $\sqrt{s_{\mathrm{NN}}} = 5$ TeV, observing a much larger enhancement at backward pseudorapidities than predicted by NPDF calculations [15]. Similar enhancements have been observed in charged-particle production at RHIC [16–19] and have been attributed to the Cronin effect [20]. The Cronin effect is often described as initial-state multiple scattering within the nucleus [21], although radial collective flow and final-state recombination could produce similar enhancements [22,23]. However, measurements of inclusive charged-particle and π^0 production at central rapidity at the LHC show no evidence of a Cronin-like enhancement [24–27], potentially pointing to interplay between enhancing effects and low-x effects such as parton saturation [28,29].

Untangling the causes of the effects observed at RHIC and the LHCb experiment requires measurements of the nuclear modification factor of identified particles, such as neutral pions, over a broad rapidity range. Multiple scattering in the nucleus would result in similar enhancements for all particle species, while radial flow is expected to have a larger transverse momentum (p_T) hardening effect on higher mass particles included in charged-particle measurements [30]. Alternatively, recombination is expected to produce a particularly large baryon enhancement [23]. The PHENIX Collaboration recently reported enhancements of π^0 production in small-collision systems, observing a system size dependence qualitatively consistent with radial flow, although still quantitatively consistent with NPDF predictions [31]. A study of π^0 production with the LHCb detector will help differentiate between contributions from nuclear parton density effects, initial-state multiple scattering, and final-state collective flow.

---

[*] Full author list given at the end of the Letter.

0031-9007/23/131(4)/042302(12)

This Letter presents a measurement of the nuclear modification factor of π^0 meson production in p-Pb collisions at $\sqrt{s_{\mathrm{NN}}} = 8.16$ TeV with the LHCb detector. The nuclear modification factor is given by

$$R_{p\text{-Pb}} \equiv \frac{1}{A} \frac{d\sigma_{p\text{-Pb}}/dp_T}{d\sigma_{pp}/dp_T}, \tag{1}$$

where $A = 208$ is the atomic mass number of the lead nucleus and $d\sigma_{p\text{-Pb}}/dp_T$ and $d\sigma_{pp}/dp_T$ are the π^0 differential production cross sections in p-Pb and proton-proton (pp) collisions, respectively. The π^0 cross section is measured in p-Pb collisions at $\sqrt{s_{\mathrm{NN}}} = 8.16$ TeV at both forward and backward rapidities relative to the proton beam. The LHCb detector collected only a small sample of unbiased pp collisions at $\sqrt{s} = 8$ TeV, hence a pp reference cross section is constructed by interpolating between measurements performed using pp collisions at $\sqrt{s} = 5$ and 13 TeV. The nuclear modification factor is measured for $1.5 < p_T < 10.0$ GeV in the pseudorapidity regions $2.5 < \eta_{\mathrm{c.m.}} < 3.5$ and $-4.0 < \eta_{\mathrm{c.m.}} < -3.0$, where $\eta_{\mathrm{c.m.}}$ is the pseudorapidity in the center-of-mass frame related to the laboratory frame pseudorapidity η_{lab} by $\eta_{\mathrm{c.m.}} = \eta_{\mathrm{lab}} - 0.465$ in p-Pb collisions and $\eta_{\mathrm{c.m.}} = \eta_{\mathrm{lab}}$ in pp collisions (natural units are used throughout this Letter).

The LHCb detector is a single-arm forward spectrometer covering the pseudorapidity range $2 < \eta_{\mathrm{lab}} < 5$, described in detail in Refs. [32,33]. The detector includes a high-precision tracking system consisting of a silicon-strip vertex detector (VELO) surrounding the interaction region, a large-area silicon-strip detector located upstream of a dipole magnet, and three stations of silicon-strip detectors and straw drift tubes placed downstream of the magnet. Photons and electrons are identified by a calorimeter system consisting of scintillating-pad and preshower detectors, an electromagnetic (ECAL) and a hadronic calorimeter. Particularly important for this analysis is the ECAL, which consists of alternating layers of lead and scintillator and has an energy (E) resolution of $13.5\%/\sqrt{E/\mathrm{GeV}} \oplus 5.2\% \oplus (0.32\ \mathrm{GeV})/E$ [34]. Simulated data samples are used to model the detector response to neutral pion reconstruction. In the simulation, p-Pb collisions are generated using EPOS-LHC [35], while pp collisions are generated using PYTHIA [36] with a specific LHCb configuration [37]. Decays of unstable particles are described by EvtGen [38] and final-state radiation is generated using PHOTOS [39]. The interaction of the generated particles with the detector, and its response, are implemented using the GEANT4 toolkit [40,41] as described in Ref. [42].

Proton-lead collisions are recorded in the forward configuration, in which the proton beam travels from the interaction region toward the spectrometer, and in the backward configuration, in which the lead ion beam travels toward the spectrometer. The forward (backward) datasets correspond to an integrated luminosity of $328 \pm 9\ \mu\mathrm{b}^{-1}$ ($267 \pm 7\ \mu\mathrm{b}^{-1}$). The forward configuration data are used to perform measurements for positive $\eta_{\mathrm{c.m.}}$, while the backward sample is used for negative $\eta_{\mathrm{c.m.}}$. All p-Pb events must have at least one reconstructed track in the VELO, while the pp samples consist of unbiased events.

Neutral pions are reconstructed using their decays to pairs of photons. To ensure that both photons are in the detector acceptance, π^0 candidates must have $2.5 < \eta_{\mathrm{lab}} < 4.0$. Photons may reach the ECAL, or they may convert to electron-positron pairs in the detector material. Photons that reach the ECAL or that convert in the material downstream of the dipole magnet are reconstructed as energy deposits (clusters) in the ECAL and are referred to as ECAL photons. Photons that convert upstream of the dipole magnet are referred to as converted photons. Only π^0 candidates reconstructed from combinations of one ECAL photon and one converted photon are considered. This reconstruction method provides better momentum resolution than ECAL photon pairs alone and does not suffer from systematic effects due to the small opening angle between π^0 decay photons. ECAL photon clusters must contain at least two ECAL cells and must be far from the extrapolated trajectories of all reconstructed tracks. Converted photons are reconstructed from pairs of good-quality tracks with $p > 2$ GeV. To minimize the effects of energy loss via bremsstrahlung radiation, only photons that convert downstream of the VELO are considered. Converted photons are required to have a small invariant mass, with a maximum that varies based on the position of the conversion vertex along the beam axis. The reconstructed converted photon momentum is also required to point to a reconstructed primary vertex. The ECAL photon must have $p_T > 400$ MeV and the converted photon must have $p_T > 500$ MeV.

An example π^0 candidate invariant mass [$M(\gamma\gamma)$] distribution in one interval of p_T and $\eta_{\mathrm{c.m.}}$ is shown in Fig. 1. The π^0 yield is determined using a binned maximum likelihood fit to the $M(\gamma\gamma)$ distribution. The π^0 signal is modeled by a two-sided Crystal Ball function [43]. The parameters describing the tails of the signal distribution are determined from simulation, while the Gaussian mean and width are left to vary in the fit to the data. The combinatorial background is modeled using charged particles as proxies for neutral pions. Charged particles reconstructed in the tracking system are given the π^0 mass, and their decays to two photons are simulated. The simulated photons are combined with reconstructed ECAL photons to form background candidates. The mass distribution of the proxy background candidates accurately describes combinatorial backgrounds in simulation and is used as a background model in the fit. An additional background component arises when a converted photon is combined with its own bremsstrahlung radiation to form a π^0 candidate, producing a peak at low mass. This background is modeled by convolving the reconstructed converted

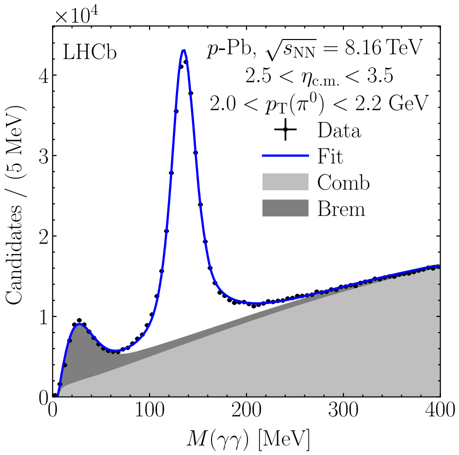

FIG. 1. Example $M(\gamma\gamma)$ distribution in forward p-Pb collisions at $\sqrt{s_{\mathrm{NN}}} = 8.16$ TeV for $2.5 < \eta_{\mathrm{c.m.}} < 3.5$ and $2.0 < p_T(\pi^0) < 2.2$ GeV. Fit results are overlaid with the total fit shown as a solid line. The combinatorial (Comb) and bremsstrahlung (Brem) backgrounds are shown as light and dark shaded regions, respectively.

photon mass distribution with the sum of two positive half-normal distributions. The width of the narrower half-normal distribution is left to vary in the fit, while the larger width is fixed using simulation.

The π^0 yields are corrected for the effects of the detector response using simulation and an iterative unfolding procedure. First, correction factors are calculated for each p_T interval from simulation and are used to correct the measured π^0 yields. The corrected π^0 spectrum in data and the true π^0 spectrum in simulation are then fit to Hagedorn functions [44]. The ratio of these fits is used to weight the true π^0 p_T spectrum in simulation. The procedure is then repeated with the weighted simulated data sample. The procedure consistently converges after three iterations.

Differences in reconstruction efficiency between data and simulation are measured and corrected for [45]. The ECAL photon reconstruction efficiency is the product of the cluster reconstruction efficiency and the photon cluster identification efficiency. The former is estimated with a tag-and-probe method using converted photons. The tag electron must be matched to an ECAL cluster and be identified as an electron. The cluster efficiency is then the fraction of probe electron tracks with a matching ECAL cluster. The photon cluster identification efficiency is evaluated by repeating the photon reconstruction without any photon cluster identification requirements in a subset of events in each data sample and measuring the fraction of π^0 mesons that pass the requirements. The converted-photon efficiency is measured using the ratio of the yields of π^0 mesons reconstructed as an ECAL photon and a converted photon to those reconstructed as two ECAL photons. This ratio is measured for $1.0 < p_T < 1.5$ GeV where ECAL photons from π^0 decays are always reconstructed as two separate clusters. The result is then combined with the measured ECAL photon efficiency correction factors to calculate a converted-photon efficiency correction. The corrected efficiencies range from about 0.5% at 1.5 GeV to about 5% at 10 GeV.

The π^0 cross section in pp collisions at $\sqrt{s} = 8.16$ TeV is estimated by interpolating between the measured pp cross sections at $\sqrt{s} = 5$ and $\sqrt{s} = 13$ TeV. The interpolation is performed independently in each p_T interval. The cross section is interpolated using the functional form $\sigma(s) = as^b$. A linear interpolation in $\sqrt{s}$ is also considered, as is a relative placement interpolation method [46]. In the latter, placement factors are calculated using simulation assuming a linear or power-law dependence of the cross section on $\sqrt{s}$. The placement factors are then applied to data to determine the interpolated cross section.

The systematic uncertainties are summarized in Table I. The largest sources of systematic uncertainty come from the interpolation between pp cross sections and the π^0 fit model. The maximum variation of interpolation results using the different pp interpolation methods is taken as the interpolation uncertainty. The fit model uncertainty is estimated by varying the default fit parameters by their uncertainties from the simulation. The variance of the resulting yields is taken as a systematic uncertainty. The fit model uncertainty also includes a contribution from the background model, which is estimated by repeating the fit using a polynomial background and taking the difference relative to the default result as a systematic uncertainty. An additional contribution to the fit model uncertainty is assigned to the yield extraction method itself by using an alternative method, where a background-only fit is performed in the mass region $[0, 50] \cup [250, 400]$ MeV. The background is then subtracted, and the background-subtracted distribution is integrated over [50,250] MeV to estimate the π^0 yield. The difference between the

TABLE I. Relative systematic and statistical uncertainties in $d\sigma/dp_T$ and $R_{p\text{-Pb}}$ in percent. The ranges correspond to the minimum and maximum values of the associated uncertainties across all p_T intervals and both $\eta_{\mathrm{c.m.}}$ regions. The $d\sigma/dp_T$ ranges cover the uncertainties for each of the p-Pb and pp samples. All sources of systematic uncertainty are fully correlated across p_T intervals.

Source	$d\sigma/dp_T$ (%)	$R_{p\text{-Pb}}$ (%)
Fit model	2.0–12.6	0.9–15.8
Unfolding	0.3–6.4	0.4–6.4
Interpolation	⋯	0.9–4.5
Material	4.0	⋯
Efficiency	1.3–1.9	1.9–2.1
Luminosity	2.0–2.6	2.2–2.3
Total systematic	5.4–15.0	4.3–7.4
Statistical	1.0–9.6	1.4–9.1

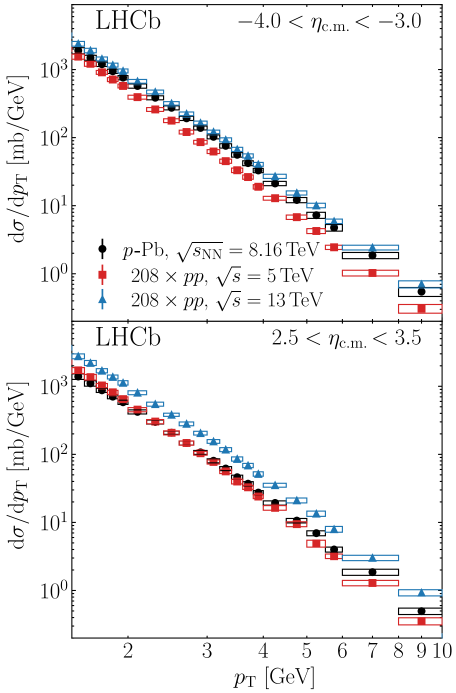

FIG. 2. Measured π^0 differential cross sections versus p_T in the (top) backward and (bottom) forward $\eta_{\mathrm{c.m.}}$ regions. Statistical uncertainties are shown by error bars, while systematic uncertainties are shown by boxes. The pp cross sections are scaled by the atomic mass of the lead ion, $A = 208$.

alternative and default yield extraction methods is taken as a systematic uncertainty.

Smaller systematic uncertainties come from unfolding, the luminosity estimate, and the efficiency correction factors. The unfolding uncertainty is estimated by using a closure test in simulation. The unfolded yields agree with the true yields in simulation to within about 1% in most p_T intervals. An additional unfolding uncertainty arises from differences in π^0 p_T resolution in data and simulation. This difference is estimated to be less than 10% by comparing the fitted widths of the π^0 peaks in data and simulation. The resolution is varied in the unfolding by ±10%, resulting in a systematic uncertainty of less than 1% in every p_T interval. The efficiency correction uncertainty arises from the finite size of the simulated data samples and results in a global uncertainty of about 1%–2%. The luminosity has been measured in pp collisions with a precision of 2% and in p-Pb collisions with a precision of 2.6% in the forward configuration and 2.5% in the backward configuration. The luminosity uncertainty is 50% correlated between datasets. The differential cross sections have an additional 4% uncertainty due to uncertainties in the detector material budget. This uncertainty is fully correlated between datasets and cancels in the nuclear modification factor.

The fully corrected π^0 differential cross sections and nuclear modification factor are shown in Figs. 2 and 3, respectively. The nuclear modification factor shows a Cronin-like enhancement at backward pseudorapidity and a strong suppression at forward pseudorapidity. These measurements are compared to next-to-leading order PQCD calculations

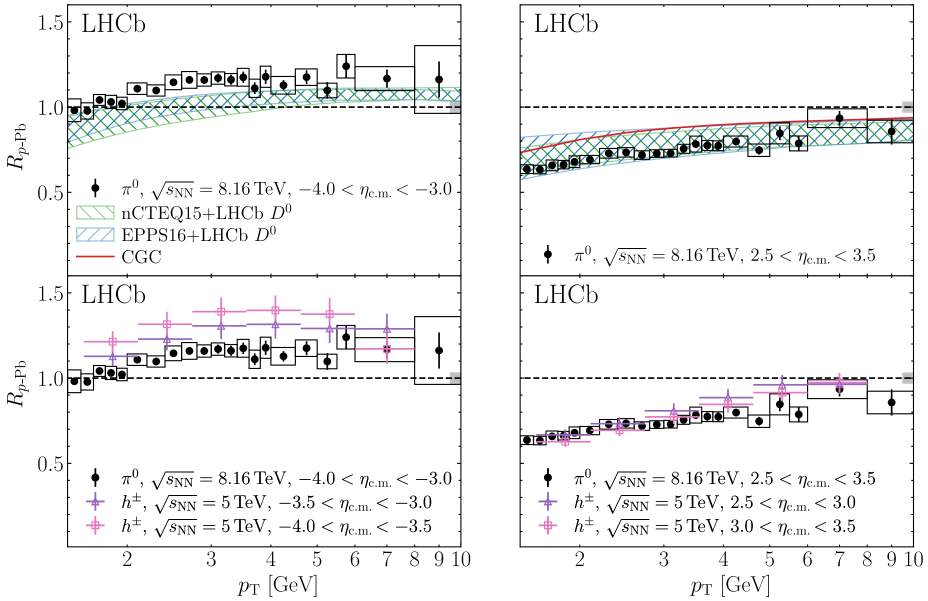

FIG. 3. Measured π^0 nuclear modification factor in the (left) backward and (right) forward $\eta_{\mathrm{c.m.}}$ regions. Error bars show the statistical uncertainty, while the open boxes show the p_T-dependent systematic uncertainties. The solid gray boxes show the overall normalization uncertainties from the luminosity estimate and efficiency correction factors. The results are compared to (top) theoretical predictions [47,49,52] and (bottom) to charged-particle data from Ref. [15]. The hatched regions show the NPDF uncertainties of the PQCD calculations. The vertical error bars on the charged-particle results show the combined systematic and statistical uncertainties.

[47] using the EPPS16 [2] and nCTEQ15 [3] NPDF sets and the DSS14 π^0 fragmentation functions [48]. The NPDFs have been reweighted to incorporate LHCb D^0 production data [49–51], resulting in considerably smaller uncertainties than calculations using the default EPPS16 and nCTEQ15 NPDFs (see Supplemental Material [51]). The measurement uncertainties in the forward region are much smaller than the NPDF uncertainties, indicating that this measurement can provide powerful constraints on NPDFs at low x. In addition, the forward results present tension with the CGC calculation [52]. The enhancement in the backward direction between 2 and 4 GeV is larger than predicted by the PQCD calculation, suggesting that effects not described by NPDFs contribute to the enhancement.

The π^0 nuclear modification factor is also compared to the charged-particle nuclear modification factor measured by the LHCb experiment in p-Pb collisions at $\sqrt{s_{\mathrm{NN}}} = 5$ TeV [15]. The forward π^0 measurement agrees with the charged-particle measurement, and the enhancement at backward $\eta_{\mathrm{c.m.}}$ is smaller than that seen for charged particles at the LHCb experiment. Because the charged-particle measurement includes heavier mesons and baryons, this ordering could indicate a mass-dependent enhancement consistent with radial flow or baryon enhancement from final-state recombination [23]. Studies of protons and heavier unflavored mesons, such as η and η' mesons, could help differentiate between these explanations.

In conclusion, the π^0 nuclear modification factor is measured at forward and backward rapidities in p-Pb collisions at $\sqrt{s_{\mathrm{NN}}} = 8.16$ TeV. The measured nuclear modification factor has a total uncertainty of less than 6% in most p_T intervals, which will provide strong constraints on models of nuclear structure and particle production in heavy ion collisions. In particular, the forward measurement is sensitive to NPDFs for x as low as 10^{-6} and can provide useful constraints in future NPDF analyses. Furthermore, the backward measurement shows the first evidence of enhanced π^0 production in proton-ion collisions at the LHC. These measurements will help constrain nuclear parton densities and models of collectivity in small-collision systems, as well as explain the origin of Cronin enhancement at the LHC.

We thank Kari Eskola, Ilkka Helenius, Heikki Mäntysaari, Petja Paakkinen, and Hannu Paukkunen for providing theoretical predictions. We express our gratitude to our colleagues in the CERN accelerator departments for the excellent performance of the LHC. We thank the technical and administrative staff at the LHCb institutes. We acknowledge support from CERN and from the national agencies: CAPES, CNPq, FAPERJ, and FINEP (Brazil); MOST and NSFC (China); CNRS/IN2P3 (France); BMBF, DFG, and MPG (Germany); INFN (Italy); NWO (Netherlands); MNiSW and NCN (Poland); MEN/IFA (Romania); MICINN (Spain); SNSF and SER (Switzerland); NASU (Ukraine); STFC (United Kingdom); DOE NP and NSF (U.S.). We acknowledge the computing resources that are provided by CERN, IN2P3 (France), KIT and DESY (Germany), INFN (Italy), SURF (Netherlands), PIC (Spain), GridPP (United Kingdom), CSCS (Switzerland), IFIN-HH (Romania), CBPF (Brazil), Polish WLCG (Poland), and NERSC (U.S.). We are indebted to the communities behind the multiple open-source software packages on which we depend. Individual groups or members have received support from ARC and ARDC (Australia); Minciencias (Colombia); AvH Foundation (Germany); EPLANET, Marie Skłodowska-Curie Actions, and ERC (European Union); A*MIDEX, ANR, IPhU, and Labex P2IO, and Région Auvergne-Rhône-Alpes (France); Key Research Program of Frontier Sciences of CAS, CAS PIFI, CAS CCEPP, Fundamental Research Funds for the Central Universities, and Science and Technology Program of Guangzhou (China); GVA, XuntaGal, GENCAT, and Prog. Atracción Talento, CM (Spain); SRC (Sweden); the Leverhulme Trust, the Royal Society, and UKRI (United Kingdom).

[1] K. Kovařík, P. M. Nadolsky, and D. E. Soper, Hadronic structure in high-energy collisions, Rev. Mod. Phys. **92**, 045003 (2020).
[2] K. J. Eskola, P. Paakkinen, H. Paukkunen, and C. A. Salgado, EPPS16: Nuclear parton distributions with LHC data, Eur. Phys. J. C **77**, 163 (2017).
[3] K. Kovařík *et al.*, nCTEQ15—Global analysis of nuclear parton distributions with uncertainties in the CTEQ framework, Phys. Rev. D **93**, 085037 (2016).
[4] D. de Florian, R. Sassot, P. Zurita, and M. Stratmann, Global analysis of nuclear parton distributions, Phys. Rev. D **85**, 074028 (2012).
[5] J. C. Collins, D. E. Soper, and G. F. Sterman, Factorization of hard processes in QCD, Adv. Ser. Dir. High Energy Phys. **5**, 1 (1989).
[6] H. Kowalski, T. Lappi, and R. Venugopalan, Nuclear Enhancement of Universal Dynamics of High Parton Densities, Phys. Rev. Lett. **100**, 022303 (2008).
[7] A. Morreale and F. Salazar, Mining for gluon saturation at colliders, Universe **7**, 312 (2021).
[8] V. Khachatryan *et al.* (CMS Collaboration), Observation of long-range near-side angular correlations in proton-proton collisions at the LHC, J. High Energy Phys. 09 (2010) 091.
[9] B. Abelev *et al.* (ALICE Collaboration), Long-range angular correlations on the near and away side in p-Pb collisions at $\sqrt{s_{NN}} = 5.02$ TeV, Phys. Lett. B **719**, 29 (2013).
[10] G. Aad *et al.* (ATLAS Collaboration), Observation of Associated Near-Side and Away-Side Long-Range Correlations in $\sqrt{s_{NN}} = 5.02$ TeV Proton-Lead Collisions with the ATLAS Detector, Phys. Rev. Lett. **110**, 182302 (2013).

[11] S. Chatrchyan *et al.* (CMS Collaboration), Observation of long-range near-side angular correlations in proton-lead collisions at the LHC, Phys. Lett. B **718**, 795 (2013).

[12] R. Aaij *et al.* (LHCb Collaboration), Measurements of long-range near-side angular correlations in $\sqrt{s_{\mathrm{NN}}} = 5$ TeV proton-lead collisions in the forward region, Phys. Lett. B **762**, 473 (2016).

[13] A. Adare *et al.* (PHENIX Collaboration), Quadrupole Anisotropy in Dihadron Azimuthal Correlations in Central $d+\mathrm{Au}$ Collisions at $\sqrt{s_{NN}} = 200$ GeV, Phys. Rev. Lett. **111**, 212301 (2013).

[14] C. Aidala *et al.* (PHENIX Collaboration), Creation of quark–gluon plasma droplets with three distinct geometries, Nat. Phys. **15**, 214 (2019).

[15] R. Aaij *et al.* (LHCb Collaboration), Measurement of the Nuclear Modification Factor and Prompt Charged Particle Production in pPb and pp Collisions at $\sqrt{s_{\mathrm{NN}}} = 5$ TeV, Phys. Rev. Lett. **128**, 142004 (2022).

[16] S. S. Adler *et al.* (PHENIX Collaboration), Absence of Suppression in Particle Production at Large Transverse Momentum in $\sqrt{s_{NN}} = 200$ GeV $d+\mathrm{Au}$ Collisions, Phys. Rev. Lett. **91**, 072303 (2003).

[17] J. Adams *et al.* (STAR Collaboration), Evidence from $d+\mathrm{Au}$ Measurements for Final State Suppression of High $p(T)$ Hadrons in $\mathrm{Au}+\mathrm{Au}$ Collisions at RHIC, Phys. Rev. Lett. **91**, 072304 (2003).

[18] I. Arsene *et al.* (BRAHMS Collaboration), Transverse Momentum Spectra in $\mathrm{Au}+\mathrm{Au}$ and $d+\mathrm{Au}$ Collisions at $\sqrt{s} = 200$ GeV and the Pseudorapidity Dependence of High $p(T)$ Suppression, Phys. Rev. Lett. **91**, 072305 (2003).

[19] C. Aidala *et al.* (PHENIX Collaboration), Nuclear-modification factor of charged hadrons at forward and backward rapidity in $p+\mathrm{Al}$ and $p+\mathrm{Au}$ collisions at $\sqrt{s_{NN}} = 200$ GeV, Phys. Rev. C **101**, 034910 (2020).

[20] J. W. Cronin *et al.*, Production of hadrons with large transverse momentum at 200, 300, and 400 GeV, Phys. Rev. D **11**, 3105 (1975).

[21] A. Accardi, Cronin effect in proton nucleus collisions: A survey of theoretical models, arXiv:hep-ph/0212148.

[22] K. S. Lee, U. W. Heinz, and E. Schnedermann, Search for collective transverse flow using particle transverse momentum spectra in relativistic heavy ion collisions, Z. Phys. C **48**, 525 (1990).

[23] R. C. Hwa and C. B. Yang, Final State Interaction as the Origin of the Cronin Effect, Phys. Rev. Lett. **93**, 082302 (2004).

[24] S. Acharya *et al.* (ALICE Collaboration), Transverse momentum spectra and nuclear modification factors of charged particles in pp, p-Pb and Pb-Pb collisions at the LHC, J. High Energy Phys. 11 (2018) 013.

[25] V. Khachatryan *et al.* (CMS Collaboration), Charged-article nuclear modification factors in PbPb and pPb collisions at $\sqrt{s_{\mathrm{NN}}} = 5.02$ TeV, J. High Energy Phys. 04 (2017) 039.

[26] S. Acharya *et al.* (ALICE Collaboration), Neutral pion and η meson production in p-Pb collisions at $\sqrt{s_{\mathrm{NN}}} = 5.02$ TeV, Eur. Phys. J. C **78**, 624 (2018).

[27] S. Acharya *et al.* (ALICE Collaboration), Nuclear modification factor of light neutral-meson spectra up to high transverse momentum in p-Pb collisions at $\sqrt{s_{\mathrm{NN}}} = 8.16$ TeV, Phys. Lett. B **827**, 136943 (2022).

[28] A. H. Rezaeian, CGC predictions for $\mathrm{p}+\mathrm{A}$ collisions at the LHC and signature of QCD saturation, Phys. Lett. B **718**, 1058 (2013).

[29] D. Kharzeev, Y. V. Kovchegov, and K. Tuchin, Cronin effect and high $p(T)$ suppression in pA collisions, Phys. Rev. D **68**, 094013 (2003).

[30] A. Ayala, E. Cuautle, J. Magnin, and L. M. Montano, Proton and pion transverse spectra at RHIC from radial flow and finite size effects, Phys. Rev. C **74**, 064903 (2006).

[31] U. A. Acharya *et al.* (PHENIX Collaboration), Systematic study of nuclear effects in $p+\mathrm{Al}$, $p+\mathrm{Au}$, $d+\mathrm{Au}$, and ${}^3\mathrm{He}+\mathrm{Au}$ collisions at $\sqrt{s_{NN}} = 200$ GeV using π^0 production, Phys. Rev. C **105**, 064902 (2022).

[32] A. A. Alves, Jr. *et al.* (LHCb Collaboration), The LHCb detector at the LHC, J. Instrum. **3**, S08005 (2008).

[33] R. Aaij *et al.* (LHCb Collaboration), LHCb detector performance, Int. J. Mod. Phys. A **30**, 1530022 (2015).

[34] C. Abellan Beteta *et al.*, Calibration and performance of the LHCb calorimeters in run 1 and 2 at the LHC, arXiv:2008.11556 [J. Instrum. (to be published)].

[35] T. Pierog, I. Karpenko, J. M. Katzy, E. Yatsenko, and K. Werner, EPOS LHC: Test of collective hadronization with data measured at the CERN Large Hadron Collider, Phys. Rev. C **92**, 034906 (2015).

[36] T. Sjöstrand, S. Mrenna, and P. Skands, A brief introduction to PYTHIA 8.1, Comput. Phys. Commun. **178**, 852 (2008).

[37] I. Belyaev *et al.*, Handling of the generation of primary events in Gauss, the LHCb simulation framework, J. Phys. Conf. Ser. **331**, 032047 (2011).

[38] D. J. Lange, The EvtGen particle decay simulation package, Nucl. Instrum. Methods Phys. Res., Sect. A **462**, 152 (2001).

[39] N. Davidson, T. Przedzinski, and Z. Was, PHOTOS interface in C++: Technical and physics documentation, Comput. Phys. Commun. **199**, 86 (2016).

[40] J. Allison *et al.* (GEANT4 Collaboration), GEANT4 developments and applications, IEEE Trans. Nucl. Sci. **53**, 270 (2006).

[41] S. Agostinelli *et al.* (GEANT4 Collaboration), GEANT4: A simulation toolkit, Nucl. Instrum. Methods Phys. Res., Sect. A **506**, 250 (2003).

[42] M. Clemencic, G. Corti, S. Easo, C. R. Jones, S. Miglioranzi, M. Pappagallo, and P. Robbe, The LHCb simulation application, Gauss: Design, evolution and experience, J. Phys. Conf. Ser. **331**, 032023 (2011).

[43] T. Skwarnicki, A study of the radiative cascade transitions between the Upsilon-prime and Upsilon resonances, Ph.D. thesis, Institute of Nuclear Physics, Krakow, 1986 [Report No. DESY-F31-86-02].

[44] A. Adare *et al.* (PHENIX Collaboration), Detailed measurement of the e^+e^- pair continuum in $p+p$ and $\mathrm{Au}+\mathrm{Au}$ collisions at $\sqrt{s_{NN}} = 200$ GeV and implications for direct photon production, Phys. Rev. C **81**, 034911 (2010).

[45] R. Aaij *et al.* (LHCb Collaboration), Measurement of the electron reconstruction efficiency at LHCb, J. Instrum. **14**, P11023 (2019).

[46] V. Khachatryan *et al.* (CMS Collaboration), Nuclear effects on the transverse momentum spectra of charged particles in pPb collisions at $\sqrt{s_{\mathrm{NN}}} = 5.02$ TeV, Eur. Phys. J. C **75**, 237 (2015).

[47] I. Helenius, K. J. Eskola, and H. Paukkunen, Probing the small-x nuclear gluon distributions with isolated photons at forward rapidities in p + Pb collisions at the LHC, J. High Energy Phys. 09 (2014) 138.

[48] D. de Florian, R. Sassot, M. Epele, R. J. Hernandez-Pinto, and M. Stratmann, Parton-to-pion fragmentation reloaded, Phys. Rev. D **91**, 014035 (2015).

[49] K. J. Eskola, I. Helenius, P. Paakkinen, and H. Paukkunen, A QCD analysis of LHCb D-meson data in p + Pb collisions, J. High Energy Phys. 05 (2020) 037.

[50] R. Aaij *et al.* (LHCb Collaboration), Study of prompt D^0 meson production in p Pb collisions at $\sqrt{s_{\rm NN}} = 5$ TeV, J. High Energy Phys. 10 (2017) 090.

[51] See Supplemental Material at http://link.aps.org/supplemental/10.1103/PhysRevLett.131.042302 for additional plots.

[52] T. Lappi and H. Mäntysaari, Single inclusive particle production at high energy from HERA data to proton-nucleus collisions, Phys. Rev. D **88**, 114020 (2013).

R. Aaij,[32] A. S. W. Abdelmotteleb,[50] C. Abellan Beteta,[44] F. Abudinén,[50] T. Ackernley,[54] B. Adeva,[40] M. Adinolfi,[48] H. Afsharnia,[9] C. Agapopoulou,[13] C. A. Aidala,[77] S. Aiola,[25] Z. Ajaltouni,[9] S. Akar,[59] K. Akiba,[32] J. Albrecht,[15] F. Alessio,[42] M. Alexander,[53] A. Alfonso Albero,[39] Z. Aliouche,[56] P. Alvarez Cartelle,[49] S. Amato,[2] J. L. Amey,[48] Y. Amhis,[11] L. An,[42] L. Anderlini,[22] M. Andersson,[44] A. Andreianov,[38] M. Andreotti,[21] D. Ao,[6] F. Archilli,[17] A. Artamonov,[38] M. Artuso,[62] K. Arzymatov,[38] E. Aslanides,[10] M. Atzeni,[44] B. Audurier,[12] S. Bachmann,[17] M. Bachmayer,[43] J. J. Back,[50] A. Bailly-reyre,[13] P. Baladron Rodriguez,[40] V. Balagura,[12] W. Baldini,[21] J. Baptista de Souza Leite,[1] M. Barbetti,[22,b] R. J. Barlow,[56] S. Barsuk,[11] W. Barter,[55] M. Bartolini,[49] F. Baryshnikov,[38] J. M. Basels,[14] G. Bassi,[29,c] B. Batsukh,[4] A. Battig,[15] A. Bay,[43] A. Beck,[50] M. Becker,[15] F. Bedeschi,[29] I. B. Bediaga,[1] A. Beiter,[62] V. Belavin,[38] S. Belin,[40] V. Bellee,[44] K. Belous,[38] I. Belov,[38] I. Belyaev,[38] G. Bencivenni,[23] E. Ben-Haim,[13] A. Berezhnoy,[38] R. Bernet,[44] D. Berninghoff,[17] H. C. Bernstein,[62] C. Bertella,[56] A. Bertolin,[28] C. Betancourt,[44] F. Betti,[42] Ia. Bezshyiko,[44] S. Bhasin,[48] J. Bhom,[35] L. Bian,[67] M. S. Bieker,[15] N. V. Biesuz,[21] S. Bifani,[47] P. Billoir,[13] A. Biolchini,[32] M. Birch,[55] F. C. R. Bishop,[49] A. Bitadze,[56] A. Bizzeti, M. Bjørn,[57] M. P. Blago,[49] T. Blake,[50] F. Blanc,[43] S. Blusk,[62] D. Bobulska,[53] J. A. Boelhauve,[15] O. Boente Garcia,[40] T. Boettcher,[59] A. Boldyrev,[38] N. Bondar,[38,42] S. Borghi,[56] M. Borisyak,[38] M. Borsato,[17] J. T. Borsuk,[35] S. A. Bouchiba,[43] T. J. V. Bowcock,[54,42] A. Boyer,[42] C. Bozzi,[21] M. J. Bradley,[55] S. Braun,[60] A. Brea Rodriguez,[40] J. Brodzicka,[35] A. Brossa Gonzalo,[50] D. Brundu,[27] A. Buonaura,[44] L. Buonincontri,[28] A. T. Burke,[56] C. Burr,[42] A. Bursche,[66] A. Butkevich,[38] J. S. Butter,[32] J. Buytaert,[42] W. Byczynski,[42] S. Cadeddu,[27] H. Cai,[67] R. Calabrese,[21,d] L. Calefice,[15,13] S. Cali,[23] R. Calladine,[47] M. Calvi,[26,e] M. Calvo Gomez,[75] P. Camargo Magalhaes,[48] P. Campana,[23] D. H. Campora Perez,[74] A. F. Campoverde Quezada,[6] S. Capelli,[26,e] L. Capriotti,[20,f] A. Carbone,[20,f] G. Carboni,[31] R. Cardinale,[24,g] A. Cardini,[27] I. Carli,[4] P. Carniti,[26,e] L. Carus,[14] A. Casais Vidal,[40] R. Caspary,[17] G. Casse,[54] M. Cattaneo,[42] G. Cavallero,[42] V. Cavallini,[21,d] S. Celani,[43] J. Cerasoli,[10] D. Cervenkov,[57] A. J. Chadwick,[54] M. G. Chapman,[48] M. Charles,[13] Ph. Charpentier,[42] C. A. Chavez Barajas,[54] M. Chefdeville,[8] C. Chen,[3] S. Chen,[4] A. Chernov,[35] V. Chobanova,[40] S. Cholak,[43] M. Chrzaszcz,[35] A. Chubykin,[38] V. Chulikov,[38] P. Ciambrone,[23] M. F. Cicala,[50] X. Cid Vidal,[40] G. Ciezarek,[42] G. Ciullo,[21,d] P. E. L. Clarke,[52] M. Clemencic,[42] H. V. Cliff,[49] J. Closier,[42] J. L. Cobbledick,[56] V. Coco,[42] J. A. B. Coelho,[11] J. Cogan,[10] E. Cogneras,[9] L. Cojocariu,[37] P. Collins,[42] T. Colombo,[42] L. Congedo,[19,h] A. Contu,[27] N. Cooke,[47] G. Coombs,[53] I. Corredoira,[40] G. Corti,[42] C. M. Costa Sobral,[50] B. Couturier,[42] D. C. Craik,[58] J. Crkovská,[61] M. Cruz Torres,[1,i] R. Currie,[52] C. L. Da Silva,[61] S. Dadabaev,[38] L. Dai,[65] E. Dall'Occo,[15] J. Dalseno,[40] C. D'Ambrosio,[42] A. Danilina,[38] P. d'Argent,[42] J. E. Davies,[56] A. Davis,[56] O. De Aguiar Francisco,[56] J. de Boer,[42] K. De Bruyn,[73] S. De Capua,[56] M. De Cian,[43] U. De Freitas Carneiro Da Graca,[1] E. De Lucia,[23] J. M. De Miranda,[1] L. De Paula,[2] M. De Serio,[19,h] D. De Simone,[44] P. De Simone,[23] F. De Vellis,[15] J. A. de Vries,[74] C. T. Dean,[61] F. Debernardis,[19,h] D. Decamp,[8] V. Dedu,[10] L. Del Buono,[13] B. Delaney,[49] H.-P. Dembinski,[15] V. Denysenko,[44] O. Deschamps,[9] F. Dettori,[27,j] B. Dey,[71] A. Di Cicco,[23] P. Di Nezza,[23] S. Didenko,[38] L. Dieste Maronas,[40] S. Ding,[62] V. Dobishuk,[46] C. Dong,[3] A. M. Donohoe,[18] F. Dordei,[27] A. C. dos Reis,[1] L. Douglas,[53] A. G. Downes,[8] M. W. Dudek,[35] L. Dufour,[42] V. Duk,[72] P. Durante,[42] J. M. Durham,[61] D. Dutta,[56] A. Dziurda,[35] A. Dzyuba,[38] S. Easo,[51] U. Egede,[63] V. Egorychev,[38] S. Eidelman,[38,a] S. Eisenhardt,[52] S. Ek-In,[43] L. Eklund,[76] S. Ely,[62] A. Ene,[37] E. Epple,[61]

S. Escher,[14] J. Eschle,[44] S. Esen,[44] T. Evans,[56] L. N. Falcao,[1] Y. Fan,[6] B. Fang,[67] S. Farry,[54] D. Fazzini,[26,e]
M. Feo,[42] A. Fernandez Prieto,[40] A. D. Fernez,[60] F. Ferrari,[20] L. Ferreira Lopes,[43] F. Ferreira Rodrigues,[2]
S. Ferreres Sole,[32] M. Ferrillo,[44] M. Ferro-Luzzi,[42] S. Filippov,[38] R. A. Fini,[19] M. Fiorini,[21,d] M. Firlej,[34]
K. M. Fischer,[57] D. S. Fitzgerald,[77] C. Fitzpatrick,[56] T. Fiutowski,[34] F. Fleuret,[12] M. Fontana,[13] F. Fontanelli,[24,g]
R. Forty,[42] D. Foulds-Holt,[49] V. Franco Lima,[54] M. Franco Sevilla,[60] M. Frank,[42] E. Franzoso,[21,d] G. Frau,[17]
C. Frei,[42] D. A. Friday,[53] J. Fu,[6] Q. Fuehring,[15] E. Gabriel,[32] G. Galati,[19,h] A. Gallas Torreira,[40] D. Galli,[20,f]
S. Gambetta,[52,42] Y. Gan,[3] M. Gandelman,[2] P. Gandini,[25] Y. Gao,[5] M. Garau,[27,j] L. M. Garcia Martin,[50]
P. Garcia Moreno,[39] J. García Pardiñas,[26,e] B. Garcia Plana,[40] F. A. Garcia Rosales,[12] L. Garrido,[39] C. Gaspar,[42]
R. E. Geertsema,[32] D. Gerick,[17] L. L. Gerken,[15] E. Gersabeck,[56] M. Gersabeck,[56] T. Gershon,[50]
L. Giambastiani,[28] V. Gibson,[49] H. K. Giemza,[36] A. L. Gilman,[57] M. Giovannetti,[23,k] A. Gioventù,[40]
P. Gironella Gironell,[39] C. Giugliano,[21,d] K. Gizdov,[52] E. L. Gkougkousis,[42] V. V. Gligorov,[13,42] C. Göbel,[64]
E. Golobardes,[75] D. Golubkov,[38] A. Golutvin,[55,38] A. Gomes,[1,l] S. Gomez Fernandez,[39] F. Goncalves Abrantes,[57]
M. Goncerz,[35] G. Gong,[3] I. V. Gorelov,[38] C. Gotti,[26] J. P. Grabowski,[17] T. Grammatico,[13]
L. A. Granado Cardoso,[42] E. Graugés,[39] E. Graverini,[43] G. Graziani, A. T. Grecu,[37] L. M. Greeven,[32]
N. A. Grieser,[4] L. Grillo,[56] S. Gromov,[38] B. R. Gruberg Cazon,[57] C. Gu,[3] M. Guarise,[21,d] M. Guittiere,[11]
P. A. Günther,[17] E. Gushchin,[38] A. Guth,[14] Y. Guz,[38] T. Gys,[42] T. Hadavizadeh,[63] G. Haefeli,[43] C. Haen,[42]
J. Haimberger,[42] S. C. Haines,[49] T. Halewood-leagas,[54] M. M. Halvorsen,[42] P. M. Hamilton,[60] J. Hammerich,[54]
Q. Han,[7] X. Han,[17] E. B. Hansen,[56] S. Hansmann-Menzemer,[17,42] L. Hao,[6] N. Harnew,[57] T. Harrison,[54]
C. Hasse,[42] M. Hatch,[42] J. He,[6,m] K. Heijhoff,[32] K. Heinicke,[15] R. D. L. Henderson,[63,50] A. M. Hennequin,[58]
K. Hennessy,[54] L. Henry,[42] J. Heuel,[14] A. Hicheur,[2] D. Hill,[43] M. Hilton,[56] S. E. Hollitt,[15] R. Hou,[7] Y. Hou,[8]
J. Hu,[17] J. Hu,[66] W. Hu,[7] X. Hu,[3] W. Huang,[6] X. Huang,[67] W. Hulsbergen,[32] R. J. Hunter,[50] M. Hushchyn,[38]
D. Hutchcroft,[54] D. Hynds,[32] P. Ibis,[15] M. Idzik,[34] D. Ilin,[38] P. Ilten,[59] A. Inglessi,[38] A. Iniukhin,[38]
A. Ishteev,[38] K. Ivshin,[38] R. Jacobsson,[42] H. Jage,[14] S. Jakobsen,[42] E. Jans,[32] B. K. Jashal,[41] A. Jawahery,[60]
V. Jevtic,[15] X. Jiang,[4,6] M. John,[57] D. Johnson,[58] C. R. Jones,[49] T. P. Jones,[50] B. Jost,[42] N. Jurik,[42]
S. Kandybei,[45] Y. Kang,[3] M. Karacson,[42] D. Karpenkov,[38] M. Karpov,[38] J. W. Kautz,[59] F. Keizer,[42]
D. M. Keller,[62] M. Kenzie,[50] T. Ketel,[33] B. Khanji,[15] A. Kharisova,[38] S. Kholodenko,[38,38] T. Kirn,[14]
V. S. Kirsebom,[43] O. Kitouni,[58] S. Klaver,[33] N. Kleijne,[29,c] K. Klimaszewski,[36] M. R. Kmiec,[36] S. Koliiev,[46]
A. Kondybayeva,[38] A. Konoplyannikov,[38] P. Kopciewicz,[34] R. Kopecna,[17] P. Koppenburg,[32] M. Korolev,[38]
I. Kostiuk,[32,46] O. Kot,[46] S. Kotriakhova, A. Kozachuk,[38] P. Kravchenko,[38] L. Kravchuk,[38] R. D. Krawczyk,[42]
M. Kreps,[50] S. Kretzschmar,[14] P. Krokovny,[38,38] W. Krupa,[34] W. Krzemien,[36] J. Kubat,[17] W. Kucewicz,[35,34]
M. Kucharczyk,[35] V. Kudryavtsev,[38,38] H. S. Kuindersma,[32] G. J. Kunde,[61] T. Kvaratskheliya,[38] D. Lacarrere,[42]
G. Lafferty,[56] A. Lai,[27] A. Lampis,[27,j] D. Lancierini,[44] J. J. Lane,[56] R. Lane,[48] G. Lanfranchi,[23]
C. Langenbruch,[14] J. Langer,[15] O. Lantwin,[38] T. Latham,[50] F. Lazzari,[29,n] M. Lazzaroni,[25] R. Le Gac,[10]
S. H. Lee,[77] R. Lefèvre,[9] A. Leflat,[38] S. Legotin,[38] P. Lenisa,[21,d] O. Leroy,[10] T. Lesiak,[35] B. Leverington,[17]
H. Li,[66] P. Li,[17] S. Li,[7] Y. Li,[4] Z. Li,[62] X. Liang,[62] T. Lin,[55] R. Lindner,[42] V. Lisovskyi,[15] R. Litvinov,[27,j]
G. Liu,[66] H. Liu,[6] Q. Liu,[6] S. Liu,[4,6] A. Lobo Salvia,[39] A. Loi,[27] R. Lollini,[72] J. Lomba Castro,[40]
I. Longstaff,[53] J. H. Lopes,[2] S. López Soliño,[40] G. H. Lovell,[49] Y. Lu,[4,o] C. Lucarelli,[22,b] D. Lucchesi,[28,p]
S. Luchuk,[38] M. Lucio Martinez,[32] V. Lukashenko,[32,46] Y. Luo,[3] A. Lupato,[56] E. Luppi,[21,d] O. Lupton,[50]
A. Lusiani,[29,c] X.-R. Lyu,[6] L. Ma,[4] R. Ma,[6] S. Maccolini,[20] F. Machefert,[11] F. Maciuc,[37] V. Macko,[43]
P. Mackowiak,[15] S. Maddrell-Mander,[48] L. R. Madhan Mohan,[48] A. Maevskiy,[38] D. Maisuzenko,[38]
M. W. Majewski,[34] J. J. Malczewski,[35] S. Malde,[57] B. Malecki,[35] A. Malinin,[38] T. Maltsev,[38,38] H. Malygina,[17]
G. Manca,[27,j] G. Mancinelli,[10] D. Manuzzi,[20] C. A. Manzari,[44] D. Marangotto,[25,q] J. F. Marchand,[8]
U. Marconi,[20] S. Mariani,[22,b] C. Marin Benito,[42] M. Marinangeli,[43] J. Marks,[17] A. M. Marshall,[48] P. J. Marshall,[54]
G. Martelli,[72,r] G. Martellotti,[30] L. Martinazzoli,[42,e] M. Martinelli,[26,e] D. Martinez Santos,[40] F. Martinez Vidal,[41]
A. Massafferri,[1] M. Materok,[14] R. Matev,[42] A. Mathad,[44] V. Matiunin,[38] C. Matteuzzi,[26] K. R. Mattioli,[77]
A. Mauri,[32] E. Maurice,[12] J. Mauricio,[39] M. Mazurek,[42] M. McCann,[55] L. Mcconnell,[18] T. H. McGrath,[56]
N. T. McHugh,[53] A. McNab,[56] R. McNulty,[18] J. V. Mead,[54] B. Meadows,[59] G. Meier,[15] D. Melnychuk,[36]
S. Meloni,[26,e] M. Merk,[32,74] A. Merli,[25,q] L. Meyer Garcia,[2] M. Mikhasenko,[69,s] D. A. Milanes,[68] E. Millard,[50]
M. Milovanovic,[42] M.-N. Minard,[8,8,a] A. Minotti,[26,e] S. E. Mitchell,[52] B. Mitreska,[56] D. S. Mitzel,[15]

A. Mödden,[15] R. A. Mohammed,[57] R. D. Moise,[55] S. Mokhnenko,[38] T. Mombächer,[40] I. A. Monroy,[68]
S. Monteil,[9] M. Morandin,[28] G. Morello,[23] M. J. Morello,[29,c] J. Moron,[34] A. B. Morris,[69] A. G. Morris,[50]
R. Mountain,[62] H. Mu,[3] F. Muheim,[52] M. Mulder,[73] K. Müller,[44] C. H. Murphy,[57] D. Murray,[56] R. Murta,[55]
P. Muzzetto,[27,j] P. Naik,[48] T. Nakada,[43] R. Nandakumar,[51] T. Nanut,[42] I. Nasteva,[2] M. Needham,[52] N. Neri,[25,q]
S. Neubert,[69] N. Neufeld,[42] P. Neustroev,[38] R. Newcombe,[55] E. M. Niel,[43] S. Nieswand,[14] N. Nikitin,[38]
N. S. Nolte,[58] C. Normand,[8,27,j] C. Nunez,[77] A. Oblakowska-Mucha,[34] V. Obraztsov,[38] T. Oeser,[14]
D. P. O'Hanlon,[48] S. Okamura,[21,d] R. Oldeman,[27,j] F. Oliva,[52] M. E. Olivares,[62] C. J. G. Onderwater,[73]
R. H. O'Neil,[52] J. M. Otalora Goicochea,[2] T. Ovsiannikova,[38] P. Owen,[44] A. Oyanguren,[41] O. Ozcelik,[52]
K. O. Padeken,[69] B. Pagare,[50] P. R. Pais,[42] T. Pajero,[57] A. Palano,[19] M. Palutan,[23] Y. Pan,[56] G. Panshin,[38]
A. Papanestis,[51] M. Pappagallo,[19,h] L. L. Pappalardo,[21,d] C. Pappenheimer,[59] W. Parker,[60] C. Parkes,[56]
B. Passalacqua,[21,d] G. Passaleva,[22] A. Pastore,[19] M. Patel,[55] C. Patrignani,[20,f] C. J. Pawley,[74] A. Pearce,[42]
A. Pellegrino,[32] M. Pepe Altarelli,[42] S. Perazzini,[20] D. Pereima,[38] A. Pereiro Castro,[40] P. Perret,[9] M. Petric,[53]
K. Petridis,[48] A. Petrolini,[24,g] A. Petrov,[38] S. Petrucci,[52] M. Petruzzo,[25] H. Pham,[62] A. Philippov,[38]
R. Piandani,[6] L. Pica,[29,c] M. Piccini,[72] B. Pietrzyk,[8] G. Pietrzyk,[11] M. Pili,[57] D. Pinci,[30] F. Pisani,[42]
M. Pizzichemi,[26,42,e] V. Placinta,[37] J. Plews,[47] M. Plo Casasus,[40] F. Polci,[13,42] M. Poli Lener,[23] M. Poliakova,[62]
A. Poluektov,[10] N. Polukhina,[38,38] I. Polyakov,[62] E. Polycarpo,[2] S. Ponce,[42] D. Popov,[6,42] S. Popov,[38]
S. Poslavskii,[38] K. Prasanth,[35] L. Promberger,[42] C. Prouve,[40] V. Pugatch,[46] V. Puill,[11] G. Punzi,[29,t] H. R. Qi,[3]
W. Qian,[6] N. Qin,[3] R. Quagliani,[43] N. V. Raab,[18] R. I. Rabadan Trejo,[6] B. Rachwal,[34] J. H. Rademacker,[48]
R. Rajagopalan,[62] M. Rama,[29] M. Ramos Pernas,[50] M. S. Rangel,[2] F. Ratnikov,[38,38] G. Raven,[33,42] M. Reboud,[8]
F. Redi,[42] F. Reiss,[56] C. Remon Alepuz,[41] Z. Ren,[3] V. Renaudin,[57] P. K. Resmi,[10] R. Ribatti,[29,c] A. M. Ricci,[27]
S. Ricciardi,[51] K. Rinnert,[54] P. Robbe,[11] G. Robertson,[52] A. B. Rodrigues,[43] E. Rodrigues,[54]
J. A. Rodriguez Lopez,[68] E. Rodriguez Rodriguez,[40] A. Rollings,[57] P. Roloff,[42] V. Romanovskiy,[38]
M. Romero Lamas,[40] A. Romero Vidal,[40] J. D. Roth,[77,77,77,a] M. Rotondo,[23] M. S. Rudolph,[62] T. Ruf,[42]
R. A. Ruiz Fernandez,[40] J. Ruiz Vidal,[41] A. Ryzhikov,[38] J. Ryzka,[34] J. J. Saborido Silva,[40] N. Sagidova,[38]
N. Sahoo,[47] B. Saitta,[27,j] M. Salomoni,[42] C. Sanchez Gras,[32] I. Sanderswood,[41] R. Santacesaria,[30]
C. Santamarina Rios,[40] M. Santimaria,[23] E. Santovetti,[31,k] D. Saranin,[38] G. Sarpis,[14] M. Sarpis,[69] A. Sarti,[30]
C. Satriano,[30,u] A. Satta,[31] M. Saur,[15] D. Savrina,[38,38] H. Sazak,[9] L. G. Scantlebury Smead,[57] A. Scarabotto,[13]
S. Schael,[14] S. Scherl,[54] M. Schiller,[53] H. Schindler,[42] M. Schmelling,[16] B. Schmidt,[42] S. Schmitt,[14]
O. Schneider,[43] A. Schopper,[42] M. Schubiger,[32] S. Schulte,[43] M. H. Schune,[11] R. Schwemmer,[42]
B. Sciascia,[23,42] A. Sciuccati,[42] S. Sellam,[40] A. Semennikov,[38] M. Senghi Soares,[33] A. Sergi,[24,g] N. Serra,[44]
L. Sestini,[28] A. Seuthe,[15] Y. Shang,[5] D. M. Shangase,[77] M. Shapkin,[38] I. Shchemerov,[38] L. Shchutska,[43]
T. Shears,[54] L. Shekhtman,[38,38] Z. Shen,[5] S. Sheng,[4,6] V. Shevchenko,[38] E. B. Shields,[26,e] Y. Shimizu,[11]
E. Shmanin,[38] J. D. Shupperd,[62] B. G. Siddi,[21,d] R. Silva Coutinho,[44] G. Simi,[28] S. Simone,[19,h] M. Singla,[63]
N. Skidmore,[56] R. Skuza,[17] T. Skwarnicki,[62] M. W. Slater,[47] I. Slazyk,[21,d] J. C. Smallwood,[57] J. G. Smeaton,[49]
E. Smith,[44] M. Smith,[55] A. Snoch,[32] L. Soares Lavra,[9] M. D. Sokoloff,[59] F. J. P. Soler,[53] A. Solomin,[38,48]
A. Solovev,[38] I. Solovyev,[38] F. L. Souza De Almeida,[2] B. Souza De Paula,[2] B. Spaan,[15,a] E. Spadaro Norella,[25,q]
E. Spiridenkov,[38] P. Spradlin,[53] F. Stagni,[42] M. Stahl,[59] S. Stahl,[42] S. Stanislaus,[57] O. Steinkamp,[44]
O. Stenyakin,[38] H. Stevens,[15] S. Stone,[62,a] D. Strekalina,[38] F. Suljik,[57] J. Sun,[27] L. Sun,[67] Y. Sun,[60] P. Svihra,[56]
P. N. Swallow,[47] K. Swientek,[34] A. Szabelski,[36] T. Szumlak,[34] M. Szymanski,[42] S. Taneja,[56] A. R. Tanner,[48]
M. D. Tat,[57] A. Terentev,[38] F. Teubert,[42] E. Thomas,[42] D. J. D. Thompson,[47] K. A. Thomson,[54] H. Tilquin,[55]
V. Tisserand,[9] S. T'Jampens,[8] M. Tobin,[4] L. Tomassetti,[21,d] X. Tong,[5] D. Torres Machado,[1] D. Y. Tou,[3]
E. Trifonova,[38] S. M. Trilov,[48] C. Trippl,[43] G. Tuci,[6] A. Tully,[43] N. Tuning,[32,42] A. Ukleja,[36] D. J. Unverzagt,[17]
E. Ursov,[38] A. Usachov,[32] A. Ustyuzhanin,[38,38] U. Uwer,[17] A. Vagner,[38] V. Vagnoni,[20] A. Valassi,[42]
G. Valenti,[20] N. Valls Canudas,[75] M. van Beuzekom,[32] M. Van Dijk,[43] H. Van Hecke,[61] E. van Herwijnen,[38]
M. van Veghel,[73] R. Vazquez Gomez,[39] P. Vazquez Regueiro,[40] C. Vázquez Sierra,[42] S. Vecchi,[21] J. J. Velthuis,[48]
M. Veltri,[22,v] A. Venkateswaran,[62] M. Veronesi,[32] M. Vesterinen,[50] D. Vieira,[59] M. Vieites Diaz,[43] H. Viemann,[70]
X. Vilasis-Cardona,[75] E. Vilella Figueras,[54] A. Villa,[20] P. Vincent,[13] F. C. Volle,[11] D. vom Bruch,[10]
A. Vorobyev,[38] V. Vorobyev,[38] N. Voropaev,[38] K. Vos,[74] R. Waldi,[17] J. Walsh,[29] C. Wang,[17] J. Wang,[5] J. Wang,[4]
J. Wang,[3] J. Wang,[67] M. Wang,[5] R. Wang,[48] Y. Wang,[7] Z. Wang,[44] Z. Wang,[3] Z. Wang,[6] J. A. Ward,[50,63]

N. K. Watson,[47] D. Websdale,[55] C. Weisser,[58] B. D. C. Westhenry,[48] D. J. White,[56] M. Whitehead,[48]
A. R. Wiederhold,[50] D. Wiedner,[15] G. Wilkinson,[57] M. K. Wilkinson,[62] I. Williams,[49] M. Williams,[58]
M. R. J. Williams,[52] F. F. Wilson,[51] W. Wislicki,[36] M. Witek,[35] L. Witola,[17] G. Wormser,[11] S. A. Wotton,[49]
H. Wu,[62] K. Wyllie,[42] Z. Xiang,[6] D. Xiao,[7] Y. Xie,[7] A. Xu,[5] J. Xu,[6] L. Xu,[3] M. Xu,[50] Q. Xu,[6] Z. Xu,[9]
Z. Xu,[6] D. Yang,[3] S. Yang,[6] Y. Yang,[6] Z. Yang,[5] Z. Yang,[60] Y. Yao,[62] L. E. Yeomans,[54] H. Yin,[7] J. Yu,[65]
X. Yuan,[62] E. Zaffaroni,[43] M. Zavertyaev,[16] M. Zdybal,[35] O. Zenaiev,[42] M. Zeng,[3] D. Zhang,[7] L. Zhang,[3]
S. Zhang,[65] S. Zhang,[5] Y. Zhang,[5] Y. Zhang,[57] A. Zharkova,[38] A. Zhelezov,[17] Y. Zheng,[6] T. Zhou,[5] X. Zhou,[6]
Y. Zhou,[6] V. Zhovkovska,[11] X. Zhu,[3] X. Zhu,[7] Z. Zhu,[6] V. Zhukov,[14,38] Q. Zou,[4,6] S. Zucchelli,[20,f]
D. Zuliani,[28] and G. Zunica[56]

(LHCb Collaboration)

[1]*Centro Brasileiro de Pesquisas Físicas (CBPF), Rio de Janeiro, Brazil*
[2]*Universidade Federal do Rio de Janeiro (UFRJ), Rio de Janeiro, Brazil*
[3]*Center for High Energy Physics, Tsinghua University, Beijing, China*
[4]*Institute of High Energy Physics (IHEP), Beijing, China*
[5]*School of Physics State Key Laboratory of Nuclear Physics and Technology, Peking University, Beijing, China*
[6]*University of Chinese Academy of Sciences, Beijing, China*
[7]*Institute of Particle Physics, Central China Normal University, Wuhan, Hubei, China*
[8]*Université Savoie Mont Blanc, CNRS, IN2P3-LAPP, Annecy, France*
[9]*Université Clermont Auvergne, CNRS/IN2P3, LPC, Clermont-Ferrand, France*
[10]*Aix Marseille University, CNRS/IN2P3, CPPM, Marseille, France*
[11]*Université Paris-Saclay, CNRS/IN2P3, IJCLab, Orsay, France*
[12]*Laboratoire Leprince-Ringuet, CNRS/IN2P3, Ecole Polytechnique, Institut Polytechnique de Paris, Palaiseau, France*
[13]*LPNHE, Sorbonne Université, Paris Diderot Sorbonne Paris Cité, CNRS/IN2P3, Paris, France*
[14]*I. Physikalisches Institut, RWTH Aachen University, Aachen, Germany*
[15]*Fakultät Physik, Technische Universität Dortmund, Dortmund, Germany*
[16]*Max-Planck-Institut für Kernphysik (MPIK), Heidelberg, Germany*
[17]*Physikalisches Institut, Ruprecht-Karls-Universität Heidelberg, Heidelberg, Germany*
[18]*School of Physics, University College Dublin, Dublin, Ireland*
[19]*INFN Sezione di Bari, Bari, Italy*
[20]*INFN Sezione di Bologna, Bologna, Italy*
[21]*INFN Sezione di Ferrara, Ferrara, Italy*
[22]*INFN Sezione di Firenze, Firenze, Italy*
[23]*INFN Laboratori Nazionali di Frascati, Frascati, Italy*
[24]*INFN Sezione di Genova, Genova, Italy*
[25]*INFN Sezione di Milano, Milano, Italy*
[26]*INFN Sezione di Milano-Bicocca, Milano, Italy*
[27]*INFN Sezione di Cagliari, Monserrato, Italy*
[28]*Università degli Studi di Padova, Università e INFN, Padova, Padova, Italy*
[29]*INFN Sezione di Pisa, Pisa, Italy*
[30]*INFN Sezione di Roma La Sapienza, Roma, Italy*
[31]*INFN Sezione di Roma Tor Vergata, Roma, Italy*
[32]*Nikhef National Institute for Subatomic Physics, Amsterdam, Netherlands*
[33]*Nikhef National Institute for Subatomic Physics and VU University Amsterdam, Amsterdam, Netherlands*
[34]*AGH - University of Science and Technology, Faculty of Physics and Applied Computer Science, Kraków, Poland*
[35]*Henryk Niewodniczanski Institute of Nuclear Physics Polish Academy of Sciences, Kraków, Poland*
[36]*National Center for Nuclear Research (NCBJ), Warsaw, Poland*
[37]*Horia Hulubei National Institute of Physics and Nuclear Engineering, Bucharest-Magurele, Romania*
[38]*Affiliated with an institute covered by a cooperation agreement with CERN*
[39]*ICCUB, Universitat de Barcelona, Barcelona, Spain*
[40]*Instituto Galego de Física de Altas Enerxías (IGFAE), Universidade de Santiago de Compostela, Santiago de Compostela, Spain*
[41]*Instituto de Fisica Corpuscular, Centro Mixto Universidad de Valencia - CSIC, Valencia, Spain*
[42]*European Organization for Nuclear Research (CERN), Geneva, Switzerland*
[43]*Institute of Physics, Ecole Polytechnique Fédérale de Lausanne (EPFL), Lausanne, Switzerland*
[44]*Physik-Institut, Universität Zürich, Zürich, Switzerland*

[45]*NSC Kharkiv Institute of Physics and Technology (NSC KIPT), Kharkiv, Ukraine*
[46]*Institute for Nuclear Research of the National Academy of Sciences (KINR), Kyiv, Ukraine*
[47]*University of Birmingham, Birmingham, United Kingdom*
[48]*H.H. Wills Physics Laboratory, University of Bristol, Bristol, United Kingdom*
[49]*Cavendish Laboratory, University of Cambridge, Cambridge, United Kingdom*
[50]*Department of Physics, University of Warwick, Coventry, United Kingdom*
[51]*STFC Rutherford Appleton Laboratory, Didcot, United Kingdom*
[52]*School of Physics and Astronomy, University of Edinburgh, Edinburgh, United Kingdom*
[53]*School of Physics and Astronomy, University of Glasgow, Glasgow, United Kingdom*
[54]*Oliver Lodge Laboratory, University of Liverpool, Liverpool, United Kingdom*
[55]*Imperial College London, London, United Kingdom*
[56]*Department of Physics and Astronomy, University of Manchester, Manchester, United Kingdom*
[57]*Department of Physics, University of Oxford, Oxford, United Kingdom*
[58]*Massachusetts Institute of Technology, Cambridge, Massachusetts 02139, USA*
[59]*University of Cincinnati, Cincinnati, Ohio 45221, USA*
[60]*University of Maryland, College Park, Maryland 20742, USA*
[61]*Los Alamos National Laboratory (LANL), Los Alamos, New Mexico 87545, USA*
[62]*Syracuse University, Syracuse, New York 13244, USA*
[63]*School of Physics and Astronomy, Monash University, Melbourne, Australia*
(associated with Institution Department of Physics, University of Warwick, Coventry, United Kingdom)
[64]*Pontifícia Universidade Católica do Rio de Janeiro (PUC-Rio), Rio de Janeiro, Brazil*
(associated with Institution Universidade Federal do Rio de Janeiro (UFRJ), Rio de Janeiro, Brazil)
[65]*Physics and Micro Electronic College, Hunan University, Changsha City, China*
(associated with Institution Institute of Particle Physics, Central China Normal University, Wuhan, Hubei, China)
[66]*Guangdong Provincial Key Laboratory of Nuclear Science, Guangdong-Hong Kong Joint Laboratory of Quantum Matter, Institute of Quantum Matter, South China Normal University, Guangzhou, China*
(associated with Institution Center for High Energy Physics, Tsinghua University, Beijing, China)
[67]*School of Physics and Technology, Wuhan University, Wuhan, China*
(associated with Institution Center for High Energy Physics, Tsinghua University, Beijing, China)
[68]*Departamento de Fisica, Universidad Nacional de Colombia, Bogota, Colombia*
(associated with Institution LPNHE, Sorbonne Université, Paris Diderot Sorbonne Paris Cité, CNRS/IN2P3, Paris, France)
[69]*Universität Bonn - Helmholtz-Institut für Strahlen und Kernphysik, Bonn, Germany*
(associated with Institution Physikalisches Institut, Ruprecht-Karls-Universität Heidelberg, Heidelberg, Germany)
[70]*Institut für Physik, Universität Rostock, Rostock, Germany*
(associated with Institution Physikalisches Institut, Ruprecht-Karls-Universität Heidelberg, Heidelberg, Germany)
[71]*Eotvos Lorand University, Budapest, Hungary*
(associated with Institution European Organization for Nuclear Research (CERN), Geneva, Switzerland)
[72]*INFN Sezione di Perugia, Perugia, Italy*
(associated with Institution INFN Sezione di Ferrara, Ferrara, Italy)
[73]*Van Swinderen Institute, University of Groningen, Groningen, Netherlands*
(associated with Institution Nikhef National Institute for Subatomic Physics, Amsterdam, Netherlands)
[74]*Universiteit Maastricht, Maastricht, Netherlands*
(associated with Institution Nikhef National Institute for Subatomic Physics, Amsterdam, Netherlands)
[75]*DS4DS, La Salle, Universitat Ramon Llull, Barcelona, Spain*
(associated with Institution ICCUB, Universitat de Barcelona, Barcelona, Spain)
[76]*Department of Physics and Astronomy, Uppsala University, Uppsala, Sweden*
(associated with Institution School of Physics and Astronomy, University of Glasgow, Glasgow, United Kingdom)
[77]*University of Michigan, Ann Arbor, Michigan 48109, USA*
(associated with Institution Syracuse University, Syracuse, New York, USA)

[a] Deceased.
[b] Also at Università di Firenze, Firenze, Italy.
[c] Also at Scuola Normale Superiore, Pisa, Italy.
[d] Also at Università di Ferrara, Ferrara, Italy.
[e] Also at Università di Milano Bicocca, Milano, Italy.
[f] Also at Università di Bologna, Bologna, Italy.
[g] Also at Università di Genova, Genova, Italy.
[h] Also at Università di Bari, Bari, Italy.
[i] Also at Universidad Nacional Autónoma de Honduras, Tegucigalpa, Honduras.
[j] Also at Università di Cagliari, Cagliari, Italy.

[k]Also at Università di Roma Tor Vergata, Roma, Italy.
[l]Also at Universidade Federal do Triângulo Mineiro (UFTM), Uberaba-MG, Brazil.
[m]Also at Hangzhou Institute for Advanced Study, UCAS, Hangzhou, China.
[n]Also at Università di Siena, Siena, Italy.
[o]Also at Central South U., Changsha, China.
[p]Also at Università di Padova, Padova, Italy.
[q]Also at Università degli Studi di Milano, Milano, Italy.
[r]Also at Università di Perugia, Perugia, Italy.
[s]Also at Excellence Cluster ORIGINS, Munich, Germany.
[t]Also at Università di Pisa, Pisa, Italy.
[u]Also at Università della Basilicata, Potenza, Italy.
[v]Also at Università di Urbino, Urbino, Italy.